Available online at www.sciencedirect.com
SCIENCE DIRECT®
C. R. Physique 5 (2004) 215–229
COMPTES RENDUS PHYSIQUE

Gas phase molecular spectroscopy/Spectroscopie moléculaire en phase gazeuse

Femtosecond Raman time-resolved molecular spectroscopy

Bruno Lavorel [a,*], Ha Tran [a,b], Edouard Hertz [a], Olivier Faucher [a], Pierre Joubert [b], Marcus Motzkus [c], Tiago Buckup [c], Tobias Lang [c], Hrvoje Skenderovi [c], Gregor Knopp [d], Paul Beaud [d], Hans M. Frey [e]

[a] *Laboratoire de physique de l'Université de Bourgogne, UMR CNRS 5027, BP 47 870, 21078 Dijon cedex, France*
[b] *Laboratoire de physique moléculaire, UMR CNRS 6624, 25030 Besançon cedex, France*
[c] *Max-Planck-Institut für Quantenoptik, 85748 Garching, Germany*
[d] *Paul Scherrer Institute, CH-5232 Villigen PSI, Switzerland*
[e] *Department for Chemistry and Biochemistry, University of Bern, CH-3012 Bern, Switzerland*

Presented by Guy Laval

Abstract

The applicability of several femtosecond time resolved non-linear coherent techniques such as Raman induced polarization spectroscopy (RIPS), degenerate four-wave mixing (DFWM) and coherent anti-Stokes Raman spectroscopy (CARS) for molecular spectroscopy is presented. All methods rely on the initial coherent excitation of molecular states producing wavepackets, whose time evolution is then measured. In the case of RIPS and DFWM only pure rotational transitions are involved, whereas in CARS vibrational states can be excited. First the methodology of concentration and temperature measurements using RIPS in gas mixtures involving N_2, CO_2, O_2, and N_2O is shown. In addition some applications are given for the two closely related techniques DFWM and CARS. DFWM is suitable to extract the rotational constants of molecules to a high accuracy as is demonstrated by measurements on CO_2 and pyrimidine, which is a biological building block. CARS can be used to study higher order molecular constants and to sensitively determine temperature in, e.g., H_2 up to 2000 K. Finally, CARS is applied for the investigation of pressure dependent lineshape models, which are important for the temperature evaluation from spectroscopic data. ***To cite this article: B. Lavorel et al., C. R. Physique 5 (2004).***

Résumé

Spectroscopie moléculaire Raman femtoseconde résolue en temps. L'application de plusieurs techniques cohérentes non-linéaires femtosecondes résolues en temps comme la spectroscopie Raman de polarisation (RIPS), le mélange dégénéré à quatre ondes (DFWM), et la spectroscopie de diffusion Raman anti-Stokes cohérente (CARS), pour la spectroscopie moléculaire est présentée. Toutes les méthodes reposent sur l'excitation cohérente initiale d'états moléculaires produisant des paquets d'ondes dont l'évolution temporelle est ensuite mesurée. Dans les cas RIPS et DFWM, seuls des états rotationnels sont impliqués, alors qu'en CARS, des états vibrationnels peuvent être excités. En premier, la méthodologie des mesures de concentration et de température utilisant la technique RIPS dans des mélanges de gaz impliquant N_2, CO_2, O_2, et N_2O est présentée. Ensuite, plusieurs applications sont données pour les deux techniques proches DFWM et CARS. La technique DFWM est apte à extraire les constantes rotationnelles de molécules avec une grande précision comme il est démontré par des mesures sur CO_2 et la pyrimidine, qui est une unité moléculaire de construction biologique. La technique CARS peut aussi être utilisée pour étudier des constantes moléculaires d'ordre supérieur et pour mesurer avec sensibilité la température dans H_2 jusqu'à 2000 K. Finalement, la technique CARS est appliquée à l'investigation de modèles de forme de raie dépendant de la pression, qui sont importants

* Corresponding author.
E-mail address: Bruno.Lavorel@u-bourgogne.fr (B. Lavorel).

1631-0705/$ – see front matter
doi:10.1016/j.crhy.2004.01.013

pour la mesure de température à partir de données spectrales. ***Pour citer cet article : B. Lavorel et al., C. R. Physique 5 (2004).***

Keywords: Femtosecond laser; Ultrafast phenomena; Non-linear coherent and time resolved spectroscopy; Rovibrational wavepacket; Pressure measurement; Thermometry

Mots-clés : Laser femtoseconde ; Phénomènes ultra-rapides ; Spectroscopie non-linéaire cohérente et résolue en temps ; Paquet d'ondes rovibrationnel ; Mesure de pression ; Thermométrie

1. Introduction

Spectroscopy techniques based on femtosecond lasers can provide information about the molecules themselves (structure, vibrational modes) through quantum beats, but also about their environment such as the density of colliding species through relaxation processes and the temperature. Among them, non-linear coherent methods have proven their powerfulness. In this paper, we shall demonstrate the strength of coherent techniques for time-resolved spectroscopy by presenting results of Raman Induced Polarization Spectroscopy (RIPS) [1], Coherent Anti-Stokes Raman Spectroscopy (CARS) [2], and Degenerate Four Wave Mixing (DFWM) [3–6]. In these processes, the time dependent response of the molecular sample is given through the induced third order non-linear polarization. They all consist in coherently exciting a superposition of rotational states belonging to a given vibration through a non-resonant stimulated Raman process, interrogated by a time delayed and phase matched probe pulse. While in RIPS and DFWM spectroscopy the initial vibration of the molecule is not changed, CARS spectroscopy exhibits a greater flexibility in monitoring the molecular dynamics.

RIPS and DFWM are methods for rotational coherence spectroscopy (RCS) [7]. After the initial excitation, the rotational superposition state exhibits quantum beats at Raman frequencies. The spectral width of the excitation laser pulse has to be broad enough to excite a manifold of rotational states. The interference between the rotational quantum beats gives rise to coherent transients occurring periodically in time with a period given by $T_R = 1/2Bc$ for linear molecules, where B is the rotational constant and c the speed of light. The transients probed by a time resolved process can be interpreted as alignment rephasing.

Beatings in the Raman polarization have been observed by Leonhardt et al. [2], using time resolved femtosecond CARS (fs-CARS). Since then, the method has been intensively used for investigation of relaxation processes in condensed phase [8,9] or molecular dynamics in gas phase [5,10]. The temporal structure in the CARS signal arises from interference between the multiple transitions covered by the bandwidth of the excitation pulses. Constructive interference (full revivals) occurs at delay times which are multiples of $T_R = 1/2\alpha_e c$, where α_e is the first order rotational anharmonicity of the potential considering only Q-branch transitions ($\Delta J = 0$) [11].

As collisions produce rotational relaxation, the recurrences undergo a decay directly related to the density of collision partners. Rotational relaxation occurs through complex mechanisms that should be considered and adequately modeled for implementation into the coherent measurement concepts. It is especially important in the case of spectroscopic temperature and pressure measurements. The feasibility of time domain fs-CARS for investigation of rotational energy transfer (RET) processes and linewidth models has been recently demonstrated [12].

The outline of the paper is the following. The application of RIPS to the measurement of physical parameters in gas mixtures is demonstrated through the determination of concentration and temperature. Then, the two closely related Four-Wave-Mixing techniques, CARS and DFWM, are described and several examples are given to demonstrate their versatility on studying molecular constants of combustion relevant molecules and biological systems, and as well as on determining sensitively temperatures up to 2000 K. Finally, CARS is shown to allow a valuable test of lineshape models used for temperature and pressure measurements in N_2.

2. Theory

2.1. RIPS

In the RIPS experiment, the anisotropy of the sample arising from alignment rephasing of the molecules excited by the pump pulse is measured by the rotation of the probe pulse polarization axis. All pulses have the same carrier frequency ω.

If an homodyne detection scheme is used, the RIPS signal delivered by the photo multiplier measuring the depolarization of the probe is:

$$I \propto \int_{-\infty}^{+\infty} \left|E_s(t)\right|^2 \mathrm{d}t, \tag{1}$$

where $E_s(t)$ is the signal electric field whose envelope is proportional to the third order nonlinear polarization $P^{(3)}(t)$:

$$\varepsilon_s(t) \propto \mathrm{i}\omega P^{(3)}(t) = \mathrm{i}\omega\varepsilon_d(t) \int_{-\infty}^{t} \left|E_p(\tau)\right|^2 R(t-\tau)\,\mathrm{d}\tau, \tag{2}$$

where $R(t-\tau)$ is the rotational molecular response. $\varepsilon_d(t)$ is the probe time envelope, and $E_p(\tau)$ is the pump electric field. The upper limit of integration in Eq. (2) can be extended to $+\infty$ if the pump-probe delay is greater than the pump pulse width Δ_p. As the stimulated Raman process is non-resonant, the molecular response is real and the rotation of polarization is due solely to birefringence. The rotational nonlinear response $R(t-\tau)$ of a linear molecule 'i' is [1,13,14]:

$$R_i(t-\tau) \propto N_i \sum_{J_i} \beta_i^2(\rho_{J_i} - \rho_{J_i'}) g_{J_i} \frac{(J_i+1)(J_i+2)}{2J_i+3} \exp\bigl(-\gamma_{J_i}(t-\tau)\bigr) \times \sin\bigl(\omega_{J_i}(t-\tau)\bigr). \tag{3}$$

Eq. (3) gives the dependence of the signal envelope with respect to the anisotropy molecular polarizability $\beta_i = (\alpha_\parallel - \alpha_\perp)_i$ and the partial gas density N_i. J_i and J_i' are the rotational quantum numbers of the S-branch Raman transition $J_i \to J_i' = J_i + 2$ of frequency $\omega_{J_i} = 4\pi c B(2J_i+3)$ (rigid rotator approximation), with B the rotational constant of the vibrational level in which quantum beats are produced. g_{J_i} is the nuclear spin degeneracy factor, and γ_{J_i} is the linewidth (HWHM, half width at half maximum) of the transition. The population density $\rho_{J_i} = \exp(-E_{J_i}/T)/Q_i$ is calculated from the rotational energy E_{J_i} and the rotational partition function Q_i. Accurate calculations may need to correct ω_{J_i} for the centrifugal distortion. Expression (1) has been evaluated for gaussian electric fields and a constant (J-independent) linewidth obtained by averaging known data over all the different J values [15].

In a molecular gas mixture, each component produces its own series of recurrences whose amplitude is proportional to its square polarizability anisotropy and its concentration. Provided that the polarizability for all the components are known, the concentrations can be determined from the total signal [16]. When transients from different molecules overlap in time, macroscopic interference occurs and gives generally more pronounced dependence with respect to the relative concentrations. The temperature dependence of the signal is mainly given by the population distribution and also by the linewidth parameters.

2.2. Four-Wave-Mixing: DFWM and CARS

2.2.1. DFWM

Degenerate four-wave mixing probes molecular states which transitions are covered by the bandwidth of the applied laser fields. For most molecules except H_2, rotational transitions are in the range of tenths of wavenumbers, depending on the rotational excitation.

The theory for femtosecond DFWM is similar to the RIPS scheme. The response of an isotropic sample is described by the third order induced electric polarization. The method monitors the evolution of this 3rd order polarization of the sample after an initial alignment of the medium. The experiment itself probes the square of the response function. The signal is dependent of the delay between the pulses and oscillates with a difference frequency of the states involved.

The intensity of the generated signal is

$$I_{\mathrm{FWM}}(t) \approx \left| \sum_{J} \sum_{\Delta J=0,\pm 2} b_J^{\Delta J} \exp\bigl[(\mathrm{i}E_J^{\Delta J}/\hbar - \Gamma)t\bigr] \right|^2, \tag{4}$$

where E is the transition energy and b is a weighting factor which includes spin statistics, degeneracy of the rotational states involved, the population difference of the states, the Placzek Teller coefficient, and the laser bandwidth. Eq. (4) is given for a linear molecule. The selection rules for symmetric and asymmetric tops include transitions $\Delta J = \pm 1$ as well.

A Fourier transform of the transients yields a power spectrum of the Raman transitions [17]. A second sequence due to the beating of Stokes with anti-Stokes signal can be observed. Weaker, but most of the time noticeable is a third sequence which is due to beating of Stokes or anti-Stokes with the pure degenerate signal $\Delta J = 0$. The latter two sequences have a maximum which corresponds to the population of the rotational levels according to the Boltzmann distribution.

Femtosecond DFWM can probe the rotational constant B, the centrifugal term D_J, the temperature and higher distortion terms of the molecule [18]. The accuracy is better than 10^{-4} for rotational constants. Neglecting the J dependence of Γ the measured temperatures are usually too high. Since collisional dephasing is more efficient for low rotational excitation (as discussed in Section 2.3), the sample therefore mimics a higher temperature for longer delays.

2.2.2. CARS

For pulse durations short compared to the time scale of the experimentally observed molecular dynamics, the intensity I_S of the CARS signal is identical with the squared response function of the medium. I_S depends on the delay time τ between the

excitation (pump/Stokes) and the probe pulse and oscillates with the difference frequencies $\omega_n - \omega_{n'}$, if ω_n, $\omega_{n'}$ are pairs of Raman-transition frequencies of the medium:

$$I_S(\tau) = \theta(\tau)\exp(-2\Gamma\tau)\left\{\sum_n b_{\omega_n}^2 + \sum_{n,n'} b_{\omega_n} b_{\omega_{n'}} \cos\left[(\omega_n - \omega_{n'})\tau\right]\right\}. \tag{5}$$

The constant Γ denotes the collisional dephasing rate given by the inverse of the dephasing time T_2. The coefficients $b_{\omega n}$ are determined by the population difference, by the multiplicity of the molecular levels, by symmetry and spin statistic considerations, and by the J-dependence of the Raman cross-sections [19]. The fast excitation response is described by the step function $\theta(\tau)$. The bandwidth and center wavelength of the laser pulses determine the character of the measured transient, or in other words, which molecular constant is seen in the transient. The simplest form of nonresonant CARS is the degenerate case ($\omega_1 = \omega_2 = \omega_3$) (also called DFWM). If the bandwidth is small compared to the vibrational spacing, only rotational transitions are induced. The transient corresponds to the well-known Rotational Coherence Spectroscopy (RCS) introduced by Felker and Zewail [7]. A linear molecule follows the rotational selection rules $\Delta J = 0, \pm 2$ for Raman excitation. Assuming the simple picture of a rigid linear rotor, the energy shifts of the Raman signal are described by:

$$F(J+2) - F(J) = 4B\left(J + \frac{3}{2}\right). \tag{6}$$

Since the transition energies are equally spaced, all beating frequencies are multiples of the rotational constant B. Thus, the interference of the transition frequencies leads to a regular sequence of sharp recurrence peaks similar to RIPS. Their temporal separation is related to the rotational constant B. The width of the peaks is determined by the number of contributing rotational levels and therefore by the temperature. For highly symmetric molecules the exchange of nuclei due to rotation exhibits an alternation of intensity of the different rotational levels (spin statistics). This information is also incorporated in the transient. For CO_2 no intensity alternation can be observed due to the missing of odd J levels. However, additional recurrences can occur for symmetric tops with pronounced spin statistics [20]. The second type of nonresonant CARS implies the excitation of vibrational wavepackets. In this case the bandwidth covers two or more vibrational levels. The beating of Stokes $\Delta v = 1$ and Rayleigh $\Delta v = 0$ contributions, described by [21]:

$$F(v+1) - F(v) = \omega_e - 2\omega_e x_e - 2\omega_e x_e v, \tag{7}$$

directly images the molecular vibrations. Here ω_e is the vibrational frequency for infinitesimal small displacements, and $\omega_e x_e$ is the vibrational anharmonicity. A signal with $\Delta J \neq 0$ can be excluded by applying a polarization sensitive setup in the magic angle configuration [1].

In the third mixed case the bandwidth of the exciting laser pulses is broad enough to cover several rotational states but too small to cover more than one vibrational state. The difference between the center wavelength of the pump and Stokes laser is equal to the first vibrational transition with $\Delta v = 1$. In the case of linear molecules the selection rules are $\Delta v = +1$ and $\Delta J = 0 \pm 2$, with a dominance of the Q-branch $\Delta J = 0$. The corresponding energies are given by the following equation:

$$F(v+1, J) - F(v, J) = \omega_e - 2\omega_e x_e(v+1) - \alpha_e J(J+1) + \beta_e J^2(J+1)^2, \tag{8}$$

where ω_e is the vibrational frequency of the Raman transitions, $\omega_e x_e$ is the vibrational anharmonicity, and α_e, β_e are the rotational anharmonicities of first and second order.

Contrary to the RCS method the rotational constant does not appear in the transients. The transient is instead determined by the dependence of the rotational energies on the vibrational state and therefore directly represents the rotational anharmonicity of the molecular potential. The contribution of the vibrational constant ω_e in Eq. (8) does not appear in the beating. The experimental data show an oscillatory behavior with a period antiproportional to α_e. If the anharmonicity is large enough, e.g., in H_2, higher terms, β_e, can also be observed.

A combination of both, DFWM and CARS yields directly the equilibrium distance B_e when the normal mode lies collinear to the moment of inertia which determines the rotational constant. This value can be directly compared to high level ab initio calculations without performing a computer intensive anharmonic vibrational analysis.

2.3. Lineshape and RET

Because of the importance of linewidth characterization in the context of temperature and concentration measurements pursued in the field of combustion diagnostics, an extensive investigation on the density dependence of optical line shapes, including collision induced rotational energy transfer (RET) has been encouraged. Once the spectroscopic lines overlap in frequency, coherent line mixing effects may lead to difficulties in the FWM-signal evaluation. Therefore sophisticated models describing the collision induced RET while comprising a variety of fitting and scaling laws, have been developed and have

to be implemented in the various measurement techniques. The phenomenological decay constant Γ in Eq. (5) then changes to a matrix $\Gamma_{jj'}$, which couples the various rotational energy levels that are affected by the collision. Hence, taking Γ out of the summation as shown in Eq. (5) is no longer a good approximation at pressures above ~ 0.5 bar considering the Q-branch $\Delta v = 1$ transitions of N_2 molecules and therefore the off-diagonal elements of the Γ-matrix contribute significantly to the signal. To account for the off diagonal elements it is convenient to keep the diagonal form of Γ, which can be achieved by using the established G-matrix formalism [22] in the time domain. Hence, the CARS signal is given by [23]:

$$I_{\mathrm{CARS}}(\tau) \propto \left| \sum_j (\mathbf{bA})_j (\mathbf{A}^{-1}\mathbf{Pb})_j \exp\left[\left(\mathrm{i}\widetilde{\omega}_j - \widetilde{\Gamma}_j\right)\tau\right] \right|^2, \tag{9}$$

where $\mathbf{P}$ is a diagonal matrix accounting for the initial population difference ($\mathbf{P}_{JJ} = \rho_{v=0,J} - \rho_{v=1,J}$) and $\mathbf{A}$ is a constructed matrix to keep the diagonal form of the total expression. The $\widetilde{\omega}_j$'s are the new shifted eigenvalues of the transition frequencies, and $\widetilde{\Gamma}_j$ is the diagonalized form of the relaxation or RET matrix Γ.

One of the most common models providing an analytic expression for the matrix elements $\Gamma_{jj'}$ is the energy corrected sudden approximation (ECS) introduced by DePristo et al. [24]. Considering the isotropic Q-branch transitions of N_2, Γ is given by

$$\Gamma_{JJ'} = (2J'+1)\frac{\rho_{J_>}}{\rho_J} \sum_L (2L+1) \begin{pmatrix} J & L & J' \\ 0 & 0 & 0 \end{pmatrix}^2 \frac{\Phi_L(\omega_{JJ'})^2}{\Phi_L(\omega_{L0})^2} Q_L, \quad J' \neq J, \tag{10}$$

$$\Gamma_{JJ} = -\sum_{J' \neq J} \Gamma_{JJ'},$$

where $J_>$ is the upper value of (J, J'). The diagonal elements of the relaxation matrix can be calculated from the off diagonal ones [25]. Nevertheless the ECS formalism requires a subset of rates Q_L which are usually the rates in or out of the lowest rotational state and which can be obtained through the experiment or modeled by using semi empirical scaling laws [26–30]. In addition, the ECS model implements an adiabatic correction term to account for finite collision durations (Φ_L) [24].

The strong influence of line mixing with respect to time delayed fs-CARS signal evaluation is shown in Fig. 1. Three N_2 fs-CARS transients at 0.2, 1 and 5 bar N_2 pressure, and a simulation of the signals (b) including and (a) not including line mixing are presented in the figure. In absence of collisions, the detected signal would constructively interfere ('rephase') after a period of $1/(2\alpha_e c) \sim 960$ ps due to the anharmonicity of the potential surface as already described in Section 1. The loss of coherence caused by collisions is determined through the inverse collision rate ($\sim T_2$) and the 'rephasing' of the signal is partially hindered. Line mixing effects, viewed in the time domain already manifest on shorter time scales than T_2 (Fig. 2) and therefore it is in many cases necessary to implement these effects for signal evaluation. Moreover, information about RET is extractable from the measured transient signals. Coherent spectroscopic methods are highly sensitive to line mixing and therefore appear to be ideal tools for investigation of RET/lineshape models in the time domain.

An essential advantage of the time resolved coherent CARS method compared to its counterpart in the frequency domain, is that the interference between resonance and nonresonance signals is restricted to the short time window of coinciding laser pulses (~ 100 fs) as depicted in the inlay of Fig. 2. In the spectrum analysis that part of the detected transients can easily be separated by the experiment and simplifies the interpretation. In the frequency domain the non-resonant contribution adds to the real part of the third order susceptibility and hence is spread over the complete detected frequency range.

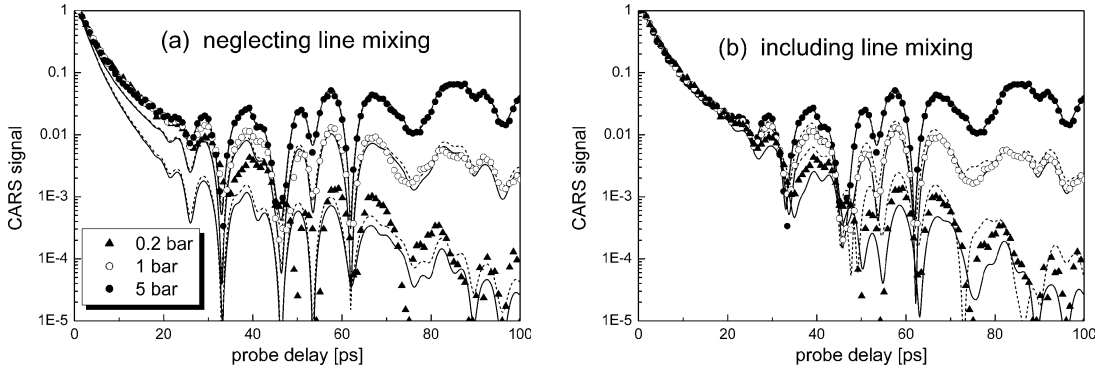

Fig. 1. Fs-CARS transients on a logarithmic scale, obtained at different N_2 pressures (0.2, 1, 5 bar). The simulation is performed by using: (a) the ECS-P scaling law not including linemixing; and (b) including linemixing considering N_2 $\Delta v = 1$ Q-branch Raman transitions.

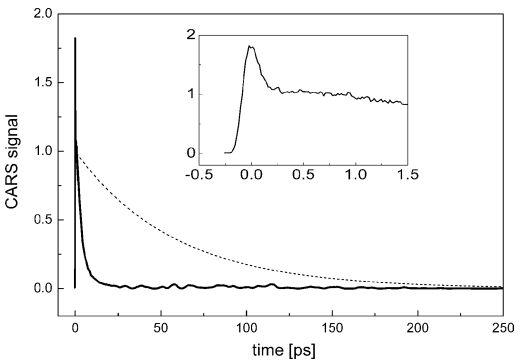

Fig. 2. Fs-CARS transient compared to the approx. inverse collision rate (exponential curve) at 1 bar pressure. The structural changes due to linemixing effects are already observable for times $< T_2$. The narrow peak at zero delay time, as shown in the inlay, is addressed to the non-resonant contribution of the signal.

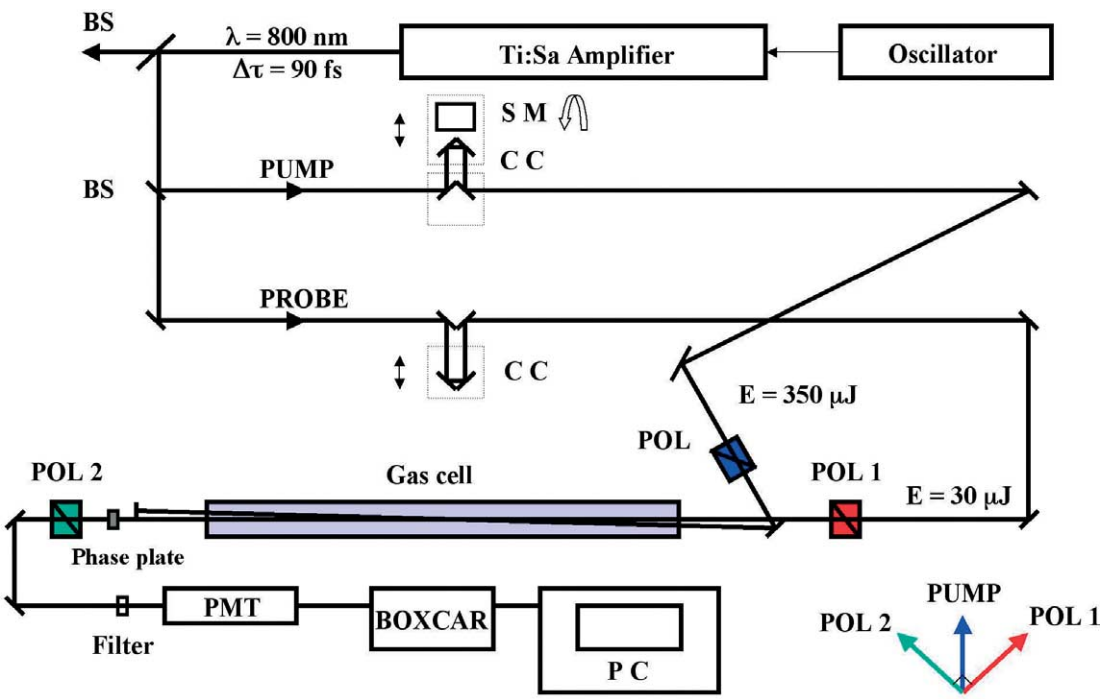

Fig. 3. Experimental setup for Raman induced polarization spectroscopy (RIPS). The probe and pump energy is given for experiment with collimated beams. The energy was decreased during the experiments performed with focused beams to avoid intensity effects. BS: beam splitter, CC: corner cube, PMT: photomultiplier tube, SM: stepping motor, POL: polarizer.

3. Experimental procedures

3.1. RIPS

The RIPS experiment is depicted in Fig. 3. The pump and probe pulses are derived from a chirped pulsed amplified (CPA) Ti:Sapphire laser system. The pulse duration is about 90 fs, the repetition rate is 20 Hz and the maximum output energy is 5 mJ. The polarization of the two pulses is defined by means of polarizers: the pump pulse is vertically polarized and the probe one is set at $+45°$. The signal field is detected by a photomultiplier through an analyzing polarizer set at $-45°$. The two beams are overlapped in a gas cell in a non-collinear configuration. The pump-probe time delay is tuned with a motorized corner cube retro-reflector. For studies at room temperature, a 1 m long gas cell has been employed and the beams were collimated. Pump and probe energy for experiments were typically 200–350 μJ and 15–30 μJ, respectively. 20 to 25 shots were accumulated at

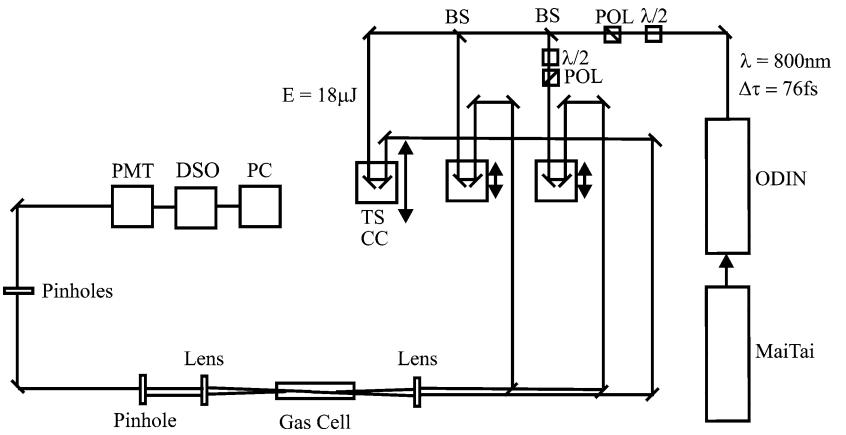

Fig. 4. Femtosecond degenerate Four-Wave mixing setup. The gas cell can be replaced by a molecular beam machine (pulsed or cw). Acronyms have the same meaning than in Fig. 3.

each pump-probe delay to improve the signal-to-noise ratio and successive steps were separated by 20–40 fs. For measurements at higher temperature, a 0.2–0.25 m long gas cell made from silica and placed in an oven was used. In that case, the two beams were focused by a lens (focal length of 0.3 m) and the energy of both was attenuated to avoid intensity effects such as alignment [31].

3.2. DFWM

Unlike above RIPS setup the DFWM setup needs two pump and one probe pulse. A schematic setup is given in Fig. 4. To satisfy phase matching, we use the folded BOXCARS configuration. The output of a CPA multipass Ti:Sa amplifier (1.6 mJ, 1 kHz @ 800 nm) is split into three pulses of equal intensity. To avoid saturation effects the beams are attenuated by means of lambda/2 polarizer sequences to 20 μJ. The beams are sent over three delay stages of which one is computer controlled. The stage has a resolution of 2 nm. The parallel polarized beams are focused into the cell or alternatively into the expansion zone of a free jet by a 700 mm lens. The generated signal is separated by a mask and the beam recollimated. After several pin holes to provide spatial filtering the signal is detected by a photomultiplier (Hamamatsu R928) with a tapered bleeder, sampled with a digital oscilloscope (LeCroy WP952) and stored on a computer. Data treatment is performed on a workstation using a Levenberg Marquart fitting routine.

3.3. CARS

The basic scheme of a CARS setup is shown in Fig. 5 [11]. The output of a commercial Ti:Sapphire femtosecond laser system with 1 kHz repetition rate, 100 fs pulse duration and 1 mJ energy per pulse was divided in two beams. One of the beams pumps an optical parametric amplifier (OPA) which is frequency doubled to deliver pulses in a spectral range of 580–730 nm at pulse energies of 10 μJ. The OPA pulse is then divided into two beams which serve as pump and probe pulse in the CARS arrangement. The Stokes pulse is provided by the second beam of the Ti:Sa output. Two of the three beams are sent via computer controlled translation stages to provide the temporal delays and then are focused together with the third beam into the sample ($f = 600$ mm) forming a folded BOXCARS configuration [5]. The generated signal then propagates in a direction which diverges from that of the incoming beams and can be easily separated by a mask and is collimated by a second lens. After spatial filtering to reduce stray light from the cell, the signal is passed through a monochromator which works as a bandpass filter and is detected with a sensitive photodetector.

For rotational CARS experiments, pump and probe were replaced by the fundamental wavelength of the Ti:Sa laser, leading to a one color setup (as in a DFWM experiment) and all three beams were s-polarized. For vibrational CARS the probe beam was at magic angle (54.7 degree) to prevent contributions of rotational CARS to the vibrational CARS signal. Strong nonresonant background, as in the case of line shift experiments on mixtures with a high percentage of foreign gas, is confined to time zero and was additionally suppressed by $+60$ degree polarization in the pump and -60 degree polarization in the signal beam, with respect to the polarization of the Stokes beam [32].

The molecules can be studied either in simple cells of fused silica at low pressures, in high pressure cells up to 100 bar or in a molecular beam.

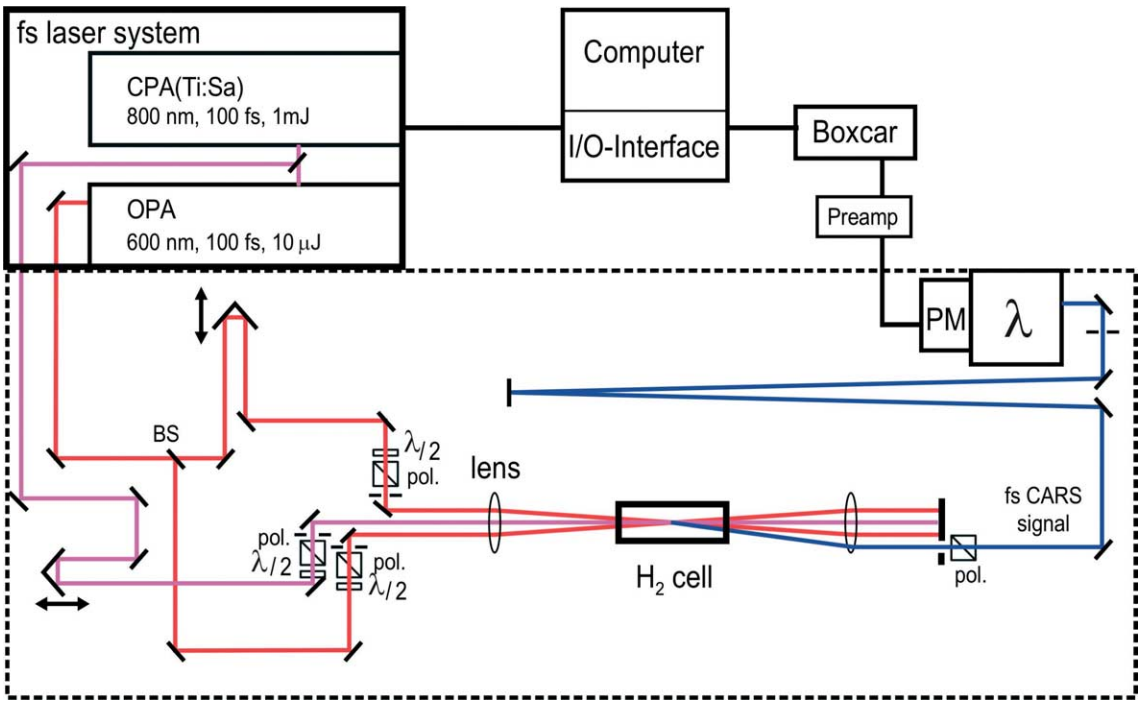

Fig. 5. Experimental setup for femtosecond CARS measurements. An additional wavelength is generated by the OPA (Optical parametric amplifier) providing pump and probe of the CARS scheme. The Stokes pulse is the fundamental of the Ti:Sa Laser system and is temporally overlapped with the pump. Acronyms have the same meaning than in Fig. 3.

4. Results

4.1. Concentration and temperature measurements using RIPS

As already discussed in Section 2.1, the concentration in a gas mixture can be extracted from the total RIPS signal. The only requirement is the knowledge of polarizability anisotropies β_i of the molecules at the laser wavelength. The procedure is based on the calculation of the signal as a function of the partial densities N_i and a least squares fitting of the data. In practice, the knowledge of ratio of polarizability anisotropies is sufficient to deduce concentrations from experiments. It has been shown that it is possible to measure concentrations in mixtures containing up to 4 components [15,16], but the method should in principle be applicable for more complex mixtures. As an example, we show in Fig. 6 an experimental trace in a N_2–CO_2–N_2O mixture. The time separation between the recurrences is 2.1 ps for N_2, 10.7 ps for CO_2 and 19.9 ps for N_2O. As these values are approximately 2, 10, 20, time overlap between the various transients occurs. The interference between overlapping transients gives rise to a modification of the total signal which strongly depends on the concentrations. This property can be exploited in order to improve the sensitivity of the measurement with respect to the concentrations. It is noted that to accurately simulate the experimental data, the pulse duration of laser pulses was set to 140 fs rather than 90 fs, to account for the loss of temporal resolution coming from the non-collinear interaction geometry. The standard deviation of the concentration measurements can be estimated from a set of experimental traces recorded in the same conditions. It is found that, in most cases, it lies in the range 0.2 to 0.4% for binary, ternary, or quaternary mixtures. The results agree well with the actual concentrations of the mixtures, generally deduced from measurements of partial and total pressures during the mixing of gases. The method can also be applied to a concentration range where the magnitudes of the relative responses of the molecular species are markedly different so that one component produces a very weak signal. In such a situation, this component cannot be measured because its contribution is embedded in the experimental noise. The solution to overcome this problem is to apply a two-pump pulse sequence in the RIPS experiment. The principle is to enhance the weak signal with respect to the total response in a given temporal window. By tuning the time delay τ between the two pump pulses and by adjusting appropriately the ratio of the intensities, the measurement becomes feasible. This method has been demonstrated in CO_2–N_2O mixture [33].

We have also explored the possibility to simultaneously measure the concentrations and temperature. As the temperature increases, more and more rotational levels are involved in the wavepacket dynamics. Consequently, the transient shape is

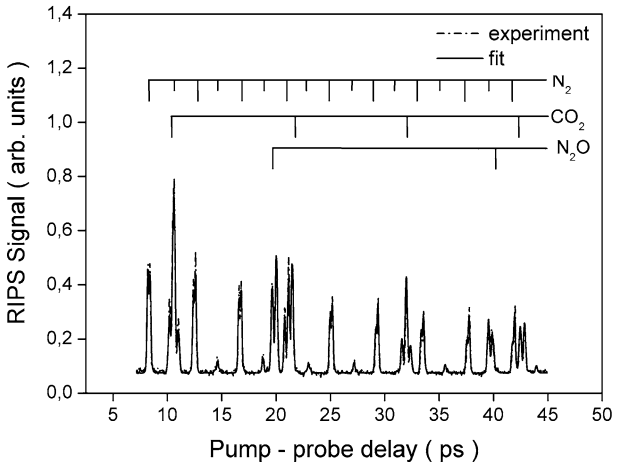

Fig. 6. Concentration measurement in a N_2O–CO_2–N_2 mixture. The pressure is $p = 1.26$ bar and temperature $T = 297$ K. The mole fractions determined from the RIPS signal are $C_{CO_2} = 0.1424$ (0.003) and $C_{N_2O} = 0.0702$ (0.003). The actual mole fractions are $C_{CO_2} = 0.1359$ (0.004) and $C_{N_2O} = 0.0709$ (0.003). The pulse duration is set to 142 fs.

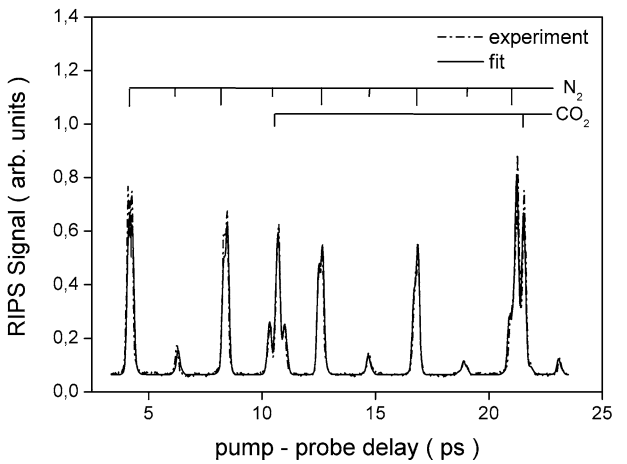

Fig. 7. Temperature and concentration measurement in a CO_2–N_2 mixture. The pressure is $p = 1.73$ bar. The temperature deduced from the RIPS experiment is $T = 592$ (20) K, whereas the CO_2 mole fractions is $C_{CO_2} = 0.1508$ (0.006). These values have to be compared to the thermocouple temperature $T_{th} = 573$ K and the actual mole fraction $C_{C0_2} = 0.1478$. The pulse duration is set to 137 fs.

modified and becomes narrower. The temperature is adjusted simultaneously with the concentration. Furthermore, if vibrational excited states are significantly populated, one must take into account their contribution to the total signal along with a slight vibrational dependence of the polarizability anisotropy. Fig. 7 shows the results obtained in a CO_2–N_2 mixture. In this situation, the temperature determined from the experimental RIPS trace is 592 K and agrees reasonably well with that given by a thermocouple (573 K). The experiments have been performed in the range 300–900 K and the results obtained seem promising for applications at higher temperature.

4.2. DFWM

In accordance with above RIPS results we will first present femtosecond DFWM of carbon dioxide in a molecular beam. To illustrate the case of an asymmetric top we will present data on pyrimidine, a molecule with relevance as building block in biological systems such as DNA.

The measurements become more accurate the longer the transient is. It is thus favorable to record long transients. However, when measuring in a gas cell, the loss of coherence due to collisions is the limiting factor. The collision rate is dependent on the density and the temperature of the sample. To avoid this restriction we moved the experiment into a molecular beam. In

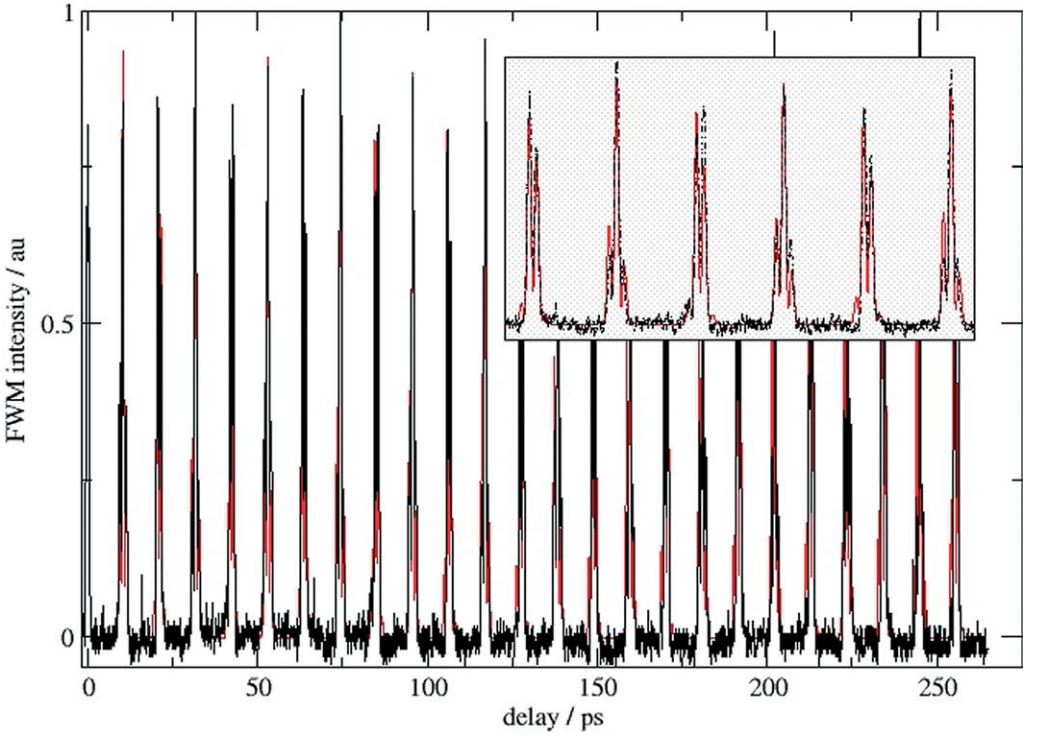

Fig. 8. Transient of CO_2 recorded in the collisionless environment of a molecular beam. Backing pressure was 1.4 bar (abs), repetition rate 20 Hz. The signal decays only when the sample leaves the probe volume (ns time scale). The fit yielded a temperature of 30 K.

Table 1
Fitted values for an expansion of CO_2 (rotational constants in cm^{-1}, temperature in K)

B_0	0.39041	$\pm 6.3 \times 10^{-6}$
D_J	-1.38×10^{-6}	$\pm 3.8 \times 10^{-7}$
Temperature	34.3	± 1.5

Fig. 8 we show a transient of CO_2 recorded in the collisionless environment of a free jet. The interaction zone was ~ 3 mm downstream the nozzle. At this distance cooling of the molecules is not completely achieved but the collision rate is sufficient low that no decay of the signal can be observed (see inset). The recurrences are at the same position and have the same shape as in the corresponding RIPS experiment.

Analysis is performed by fitting the transient to a simulation according to Eq. (4). CO_2 has a ground $^1\Sigma_g^+$ state. Due to spin statistics only transitions with $\Delta J = \pm 2$ are allowed and we used the following Placzek–Teller coefficients:

$$b_{J\to J+2} = \frac{3(J+1)(J+2)}{2(2J+1)(2J+3)}, \tag{11a}$$

$$b_{J\to J-2} = \frac{3(J-1)}{2(2J+1)(2j-1)}. \tag{11b}$$

Free parameters were the rotational constant B_0, the centrifugal term D_J, the temperature, offsets for time and intensity and an intensity scaling. In Table 1 we present the data obtained.

As an example for an asymmetric top we show data of pyrimidine recorded in a heated gas cell. Differently substituted pyrimidines form molecular building blocks of DNA and RNA and are involved in key genetic processes such as DNA replication, transcription and translation to proteins.

In Fig. 9 we show the transient recorded at a cell temperature of 343 K which results in a pressure of 5 Torr (Baratron measurement).

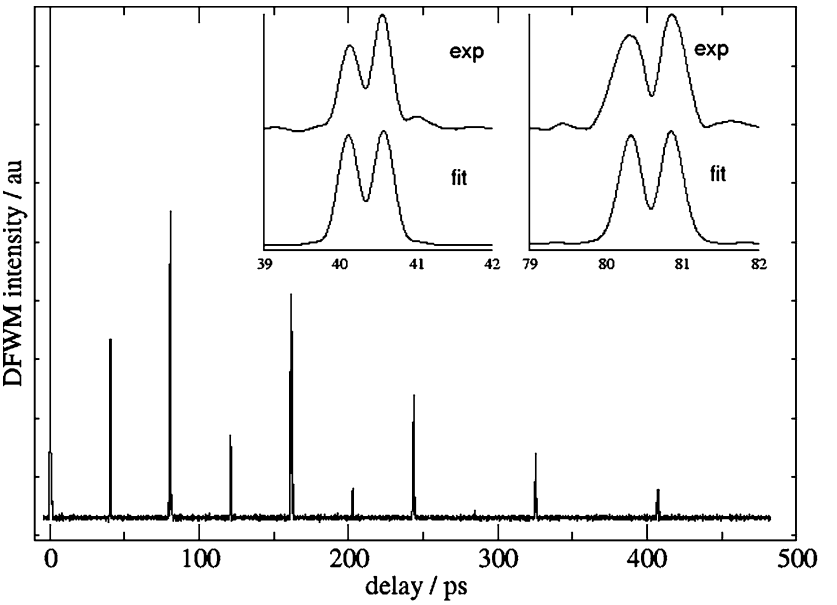

Fig. 9. DFWM transient of pyrimidine. The transients shows the typical recurrences for an asymmetric top at the oblate limit. Collisional dephasing linit the length of the transient to 500 ps. The insets show experimental and fitted curves for selected recurrences.

The energy levels of an asymmetric top close to the oblate limit can be described as

$$E(J,K) = 0.5(A+B)J(J+1) + \left[C - 0.5(A+B)\right]K^2. \tag{12}$$

The levels obtained with above formula are not accurate enough for the simulation of the transient. To obtain a good agreement between theory and data we have to setup the rotational Hamiltonian and solve the eigenvalue equation. The matrix for the Hamiltonian is constructed according to Kroto, tridiagonalized and the eigenvalues are determined. According to the selection rules for an asymmetric top, $\Delta J = 0, \pm 1, \pm 2$ and $\Delta K = 0$, we calculate the transient and fit the constants. The exact shape of the transients cannot be reproduced as we do not include centrifugal distortion. A fitting program which uses Watson's Hamiltonian has been developed in our laboratories.

From the fits we obtain the following constants:

$$A_0 = 0.2091 \pm 0.003 \text{ cm}^{-1}, \qquad B_0 = 0.2026 \pm 0.007 \text{ cm}^{-1}.$$

From our analysis we could not obtain values for the smallest constant C. At the laser intensity we used, there were no C-transients observable. Increasing the intensity resulted in background with distorted transients. This nonresonant background is probably related to the permanent alignment of molecules discussed in [31]. The DFWM signal is heterodyned with the background and the transient shapes are strongly altered.

4.3. Spectroscopy and determination of temperatures with CARS

Fig. 10 shows a theoretical CARS transient for H_2 at 3 bar, $T = 296$ K and the corresponding experimental data [11,34]. As the energies of the Raman transitions involved are not exactly commensurate, the quantum beat patterns are shifted slightly at each recurrence. At large time delays between pump/Stokes- and probe pulse the shape of the beating pattern has changed completely. In comparison to typical RCS experiments, where the signal is periodical with $T_{\text{RCS}} = 1/(2B_e c)$, the cycle duration for the signal in our fs CARS experiment is $T_{\text{CARS}} = 1/2\alpha_e c$. At times $t = n \cdot T_{\text{CARS}}$ all cosine terms of Eq. (5) are equal to 1, and apart from the exponential decay the signal reaches the same amplitude as for $t = 0$. In the case of H_2, however, the first order approximation for the rovibrational levels has to be extended to higher powers of $v + 1/2$ and $J(J+1)$, and the duration T_{CARS} between the prominent recurrences can no longer be assigned to a single molecular constant. In this case the relation $T_{\text{CARS}} \approx 1/2\alpha_e c$ only holds approximately.

This sensitivity on the higher order of constants in the femtosecond time domain can be used to determine molecular constants with high accuracy [34]. On the other hand, if the constants are well known then it is possible to utilize fs-CARS for the determination of temperatures [11]. In combustion environments the H_2 molecule is a widely used candidate for thermometry studies and single vibrational Q-branch lines as well as pure rotational levels of H_2 have been used to determine temperatures.

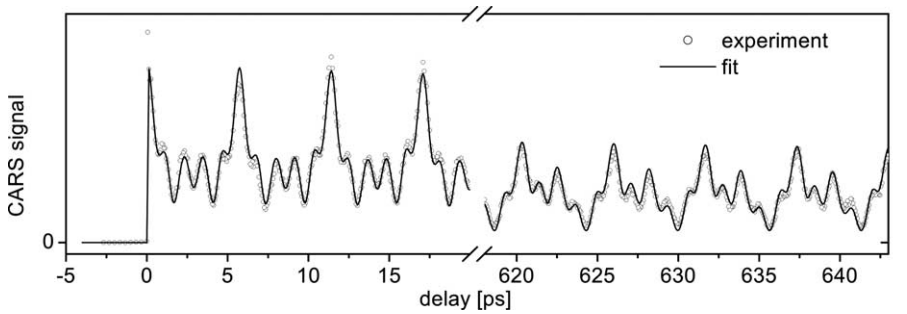

Fig. 10. Time-resolved CARS signal of H_2 molecule and theoretically predicted behavior.

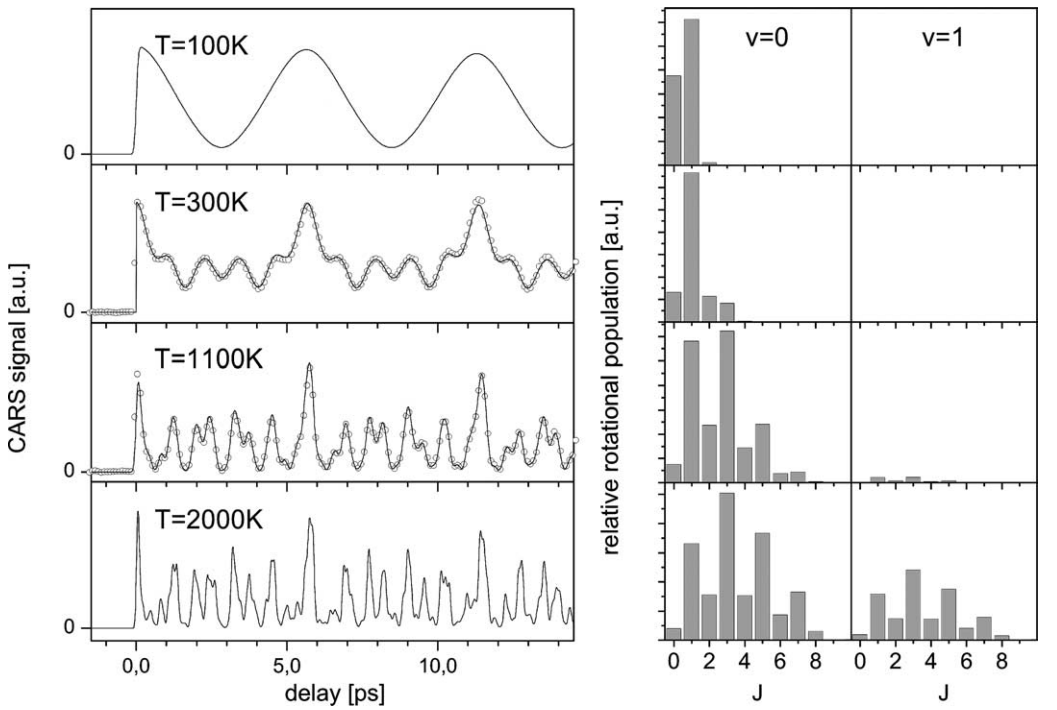

Fig. 11. CARS spectroscopy in the time-domain applied for the determination of temperature: (left) fs CARS transients on H_2 and (right) corresponding rotational population distribution at different temperatures.

Since the vibrational fs-CARS configuration probes the entire ground state Q-branch $\Delta v = 1$, $\Delta J = 0$, all populated levels contribute to the nonresonant time domain CARS signal. The probed transitions of the Q-branch differ only by the anharmonicity which allows for an excitation of all rotational levels even when the bandwidth of the laser is small compared to the Boltzmann distribution.

In a first approximation the signal is described by the molecular constant α_e yielding the cycle duration $t = 1/(2\alpha_e c)$ and the parameter $d = kT/B_e$ which describes the modulation depth of the transients [11]. In the case of weakly modulated signals (d of the order of 10 or smaller) no further corrections have to be included, and the determination of the single parameter d already allows for the measurement of temperatures with high resolution. At high temperatures and in the case of closely spaced vibrational levels, the population of the vibrational state $v = 1$ is not negligible, and the pure vibrational anharmonicity $\omega_e x_e$ has to be taken into account.

In the case of H_2 the CARS signal depends only weakly on collision induced line broadening. Therefore collisional dephasing effects are neglected. Collision induced line shifts are also hardly measurable since the energy dependent spreading of the beating pattern accumulates only at longer pump-probe delay times and are negligible at small time delays. A change of the rotational population distribution instead influences the transient from the outset. Due to the time-resolved CARS modulation, it is therefore possible to measure both, the population distribution and the temperature independently of line shape and shifts.

Fig. 11 demonstrates the strong dependence of the CARS transient on the rotational distribution. The four transients correspond to temperatures of 100, 300, 1100, and 2000 K. The simulations are based on the relative rotational distributions which are determined by the Boltzmann distribution and the spin factors and are shown in the right part of the figure. Two experimental transients for 300 and 1100 K are also given in the figure which are in excellent agreement with the theoretical curves. In all cases, the statistical error was below 1 K. In addition, the temperature was measured by means of a thermocouple which was mounted inside the oven next to the cell. The deviation was 2 K at room temperature and only 20 K at $T = 1100$ K. Nitrogen, the other prominent species for flame thermometry has recently been studied elsewhere [35] and is also discussed below.

4.4. Pressure dependency of spectroscopy and thermometry with fs-CARS

Investigations in combustion research commonly use the N_2 molecule for thermometry studies and single vibrational Q-branch lines have been used to determine temperatures and concentrations. The N_2 molecule is generally chosen because of its high availability and its simplicity in structure compared to other species involved in combustion processes. Hence, thermometry by, e.g., CARS spectroscopy is expected to be a straightforward task. As combustion research tends to show more interest in high pressure environments, the correct choice of lineshape models, incorporating collision induced energy transfer effects, become more important.

Different types of scaling models as energy corrected (ECS-E), power corrected (ECS-P), energy and frequency corrected (EFCS), and angular momentum and energy corrected (AECS) (the reader is referred, e.g., to the brief overview in [23] and references therein) variants of the ECS model can be used for a signal simulation. Interestingly at low pressures < 0.5 bar all models are sufficient in signal simulation and results on temperature or concentration evaluation are of the same quality.

However, the various RET-models strongly differ in their predictions with regard to high pressures. The fs-CARS method now allows a straightforward test of the models up to several bars. Here we will compare the ECS-P and ECS-E models. Since for more than two decades both models are prominently used in combustion diagnostics. A best data fit and a simulation with published parameter values [36,37] comparing, e.g., the two common versions of the ECS scaling law on 5 bar N_2 fs-CARS transient are given in Fig. 12. The ECS-P (a) simulation (dotted line) quite departs from the measured data. Adjusting the model parameters to the fs-CARS experiment (straight line) drastically reduces the least squared error value and a significant change of the free fit parameters is observed [23]. Fit and simulation for ECS-E scaling (Fig. 12(b)) do not differ as much as for the previous case and in general characterize the experimental data in a much better way. This behavior is also evident when the fs-CARS method is applied to determine temperature or pressure.

Using these optimized set of RET parameters for each of the two models and fitting the temperature or pressure, yields significant different results already at pressures above 2 bar. In Fig. 13 fitted pressure and temperature values from fs-CARS transients are shown. The reference pressure on the abscissa were measured with a 'Baratron' manometer ($\Delta p/p < 5\%$). The comparison of the ECS-P and ECS-E models clearly shows that in case of the N_2–N_2 collision system, the ECS-E scaling performs essentially better in prediction of temperature (room temperature of approximately 294.5 K) and pressure at absolute pressure values > 2 bar. Very impressive is that the evaluation of fs-CARS signals using the ECS-E scaling lead to $T = 294.7$ K with a standard deviation less than 3% over the whole pressure range. Based on the accuracy of the fs-CARS method and the results obtained for N_2 and other collision systems a new concept was recently introduced into the RET theory, namely that at high temperatures the energy transfer process is mainly limited by the amount of transferred angular momentum rather than by the available kinetic energy [29,30].

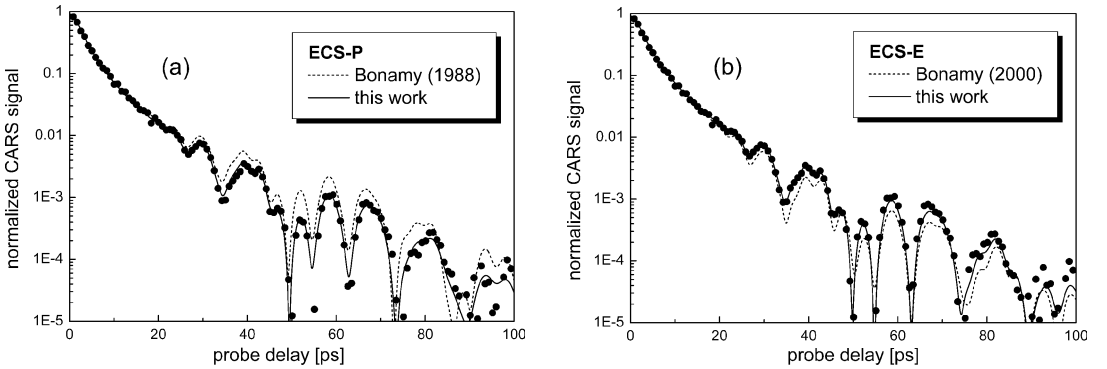

Fig. 12. Fs-CARS transients obtained at 5 bar N_2 pressure. The simulated (dotted lines) and fitted curves are shown, using: (a) the ECS-P; and (b) the ECS-E scaling model for description of the RET induced lineshapes.

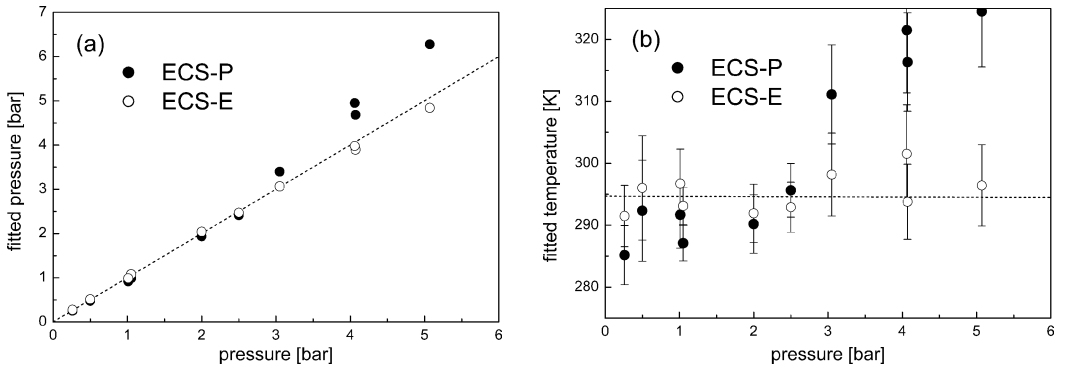

Fig. 13. (a) Fitted fs-CARS N_2 pressures by using the ECS-P and the ECS-E scaling model. The pressure values on the abscissa are detected with a manometer; (b) room temperature fit results using a pressure and temperature fit simultaneously.

5. Conclusion

Three time-resolved non-linear coherent techniques have been applied to molecular spectroscopy. First, Raman induced polarization spectroscopy related to rotational quantum beats has been used to measure concentrations and temperature in gas mixtures. The typical standard deviation of the concentration measurements is of the order of 0.3%. It is expected that this technique will be a valuable tool for non-invasive diagnostic in combustion media. Second, non-resonant femtosecond DFWM and CARS has been presented with respect to their applicability to high resolution spectroscopic studies for combustion relevant molecules as well as biological systems. Rotational constants as well as the centrifugal distortion terms can be determined with high accuracy for symmetric and asymmetric tops. The transients incorporate also information about spin statistics and therefore the symmetry of the molecule. Furthermore, we showed that fs-CARS could be used with high accuracy for thermometry studies under extreme conditions. Finally, it has been demonstrated that fs-CARS is highly sensitive to collision-induced pressure-dependent changes in optical line shapes especially when line mixing occurs and frequency resolved measurements come to their limits. This property makes fs-CARS an ideal tool for the investigation of RET models. The quantitative description of collision induced energy transfer processes, that accounts for signal dephasing in the time domain and line broadening and mixing effects in the frequency domain, is a key issue for the accuracy of many spectroscopic applications.

Acknowledgements

The authors would like to thank R. Saint-Loup and R. Chaux, for their help in this work. The continuous and generous support of Prof. K.-L. Kompa is gratefully acknowledged and the Conseil Régional de Bourgogne and the CNRS are acknowledged for their financial support. The Reaction Analysis group at the PSI is acknowledged for fruitful discussions and the Swiss federal office of energy for financial support. H. Frey acknowledges financial support from the Swiss National Science Foundation (Project: 2000021-102030/1).

References

[1] M. Morgen, W. Price, L. Hunziker, P. Ludowise, M. Blackwell, Y. Chen, Chem. Phys. Lett. 209 (1993) 1.
[2] R. Leonhardt, W. Holzapfel, W. Zinth, W. Kaiser, Chem. Phys. Lett. 133 (1987) 373.
[3] W. Zinth, W. Kaiser, in: Topics Appl. Phys., vol. 60, Springer, Berlin, 1988, p. 235.
[4] S. Mukamel, Principles of Nonlinear Optical Spectroscopy, Oxford University Press, Oxford, 1995.
[5] M. Motzkus, S. Pedersen, A.H. Zewail, J. Phys. Chem. 100 (1996) 5620.
[6] A.M. Zheltikov, J. Raman Spectrosc. 31 (2000) 653.
[7] P.M. Felker, A.H. Zewail, in: J. Manz, L. Wöste (Eds.), in: Femtosecond Chemistry, vol. 1, VCH, Weinheim, 1995.
[8] M. Fickenscher, H.G. Purucker, A. Laubereau, Chem. Phys. Lett. 191 (1992) 182.
[9] T. Chen, A. Vierheilig, P. Waltner, M. Heid, A. Materny, Chem Phys. Lett. 325 (2000) 176.
[10] M. Schmitt, G. Knopp, A. Materny, W. Kiefer, Chem. Phys. Lett. 270 (1997) 9.
[11] T. Lang, K.L. Kompa, M. Motzkus, Chem. Phys. Lett. 310 (1999) 65.
[12] G. Knopp, P. Beaud, P.P. Radi, M. Tulej, B. Bougie, D. Cannavo, T. Gerber, J. Raman Spectrosc. 33 (2002) 861.
[13] M. Morgen, W. Price, P. Ludowise, Y. Chen, J. Chem. Phys. 102 (1995) 8780.

[14] B. Lavorel, O. Faucher, M. Morgen, R. Chaux, J. Raman Spectrosc. 31 (2000) 77.
[15] H. Tran, B. Lavorel, O. Faucher, R. Saint Loup, P. Joubert, J. Raman Spectrosc. 33 (2002) 872.
[16] E. Hertz, B. Lavorel, O. Faucher, R. Chaux, J. Chem. Phys. 113 (2000) 6629.
[17] H.-M. Frey, P. Beaud, T. Gerber, B. Mischler, P.P. Radi, A.P. Tzannis, Appl. Phys. B 68 (1999) 735.
[18] H.-M. Frey, P. Beaud, T. Gerber, B. Mischler, P.P. Radi, A.P. Tzannis, J. Raman Spectrosc. 31 (2000) 71.
[19] H.W. Schrötter, H.W. Klöckner, in: Topics Current Phys., vol. 11, Springer, Berlin, 1979, p. 123.
[20] H. Frey, D. Kummli, S. Leutwyler, in preparation.
[21] G. Herzberg, in: Spectra of Diatomic Molecules, vol. 1, Molecular Spectra and Molecular Structure, second ed., Krieger, Florida, 1950.
[22] M.L. Koszykowski, R.L. Farrow, R.E. Palmer, Opt. Lett. 10 (1985) 478.
[23] G. Knopp, P. Radi, M. Tulej, T. Gerber, P. Beaud , J. Chem. Phys. 118 (2003) 8223.
[24] A.E. DePristo, S.D. Augustin, R. Ramaswamy, H. Rabitz, J. Chem. Phys. 71 (1979) 850.
[25] A. Ben-Reuven, Phys. Rev. 141 (1966) 34.
[26] T.A. Brunner, R.D. Driver, N. Smith, D.E. Pritchard, Phys. Rev. Lett. 41 (1978) 856.
[27] J.C. Polanyi, K.B. Woodall, J. Chem. Phys. 56 (1972) 1563.
[28] I. Procaccia, R.D. Levine, J. Chem. Phys. 64 (1976) 808.
[29] P. Beaud, G. Knopp, Chem. Phys. Lett. 371 (2003) 194.
[30] P. Beaud, T. Gerber, P.P. Radi, M. Tulej, G. Knopp, Chem. Phys. Lett. 373 (2003) 251.
[31] V. Renard, M. Renard, S. Guerin, Y.T. Pashayan, B. Lavorel, O. Faucher, H.R. Jauslin, Phys. Rev. Lett. 90 (2003) 153601.
[32] S.A. Akhmanov, A.F. Bunkin, S.G. Ivanov, N.I. Koroteev, Sov. Phys. JETP 47 (1978) 667.
[33] E. Hertz, R. Chaux, O. Faucher, B. Lavorel, J. Chem. Phys. 115 (2001) 3598.
[34] T. Lang, M. Motzkus, H.M. Frey, P. Beaud, J. Chem. Phys. 115 (2001) 5418.
[35] P. Beaud, H.M. Frey, T. Lang, M. Motzkus, Chem. Phys. Lett. 344 (2001) 407.
[36] L. Bonamy, J. Bonamy, D. Robert, B. Lavorel, R. Saint-Loup, R. Chaux, J. Santos, H. Berger, J. Chem. Phys. 89 (1988) 5568.
[37] L. Bonamy, J.V. Buldyreva, Phys. Rev. A 63 (2000) 012715.